



Activation of cDCs and iNKT cells contributes to triptolide-induced hepatotoxicity via STING signaling pathway and endoplasmic reticulum stress

Xin Chen · Zixun Yu · Cheng Nong · Rufeng Xue · Mingxuan Zhang ·
Yiyang Zhang · Lixin Sun · Luyong Zhang · Xinzhi Wang

Received: 11 June 2022 / Accepted: 11 November 2022
© The Author(s), under exclusive licence to Springer Nature B.V. 2022

Abstract Triptolide (TP) exhibits therapeutic potential against multiple diseases. However, its application in clinics is limited by TP-induced hepatotoxicity. TP can activate invariant natural killer T (iNKT) cells in the liver, shifting Th1 cytokine bias to Th2 cytokine bias. The damaging role of iNKT cells in TP-induced hepatotoxicity has been established, and iNKT cell deficiency can mitigate hepatotoxicity. However, the activation of iNKT cells in vitro by TP requires the presence

of antigen-presenting cells. Therefore, we hypothesized that TP could induce dendritic cells (DCs) to activate iNKT cells, thereby leading to hepatotoxicity. The hepatic conventional DCs (cDCs) exhibited immunogenic activities after TP administration, upregulating the expression of CD1d, co-stimulatory molecules, and IL-12. Neutralization with IL-12p40 antibody extenuated TP-induced hepatotoxicity and reduced iNKT cell activation, suggesting that IL-12 could cause liver injury by activating iNKT cells. TP triggered the activation and upregulation of STING signaling pathway and increased endoplasmic reticulum (ER) stress. Downregulation of STING reduced cDC immunogenicity, inhibiting the activation of iNKT cells and hepatic damage. These indicated the regulatory effects of STING pathway on cDCs and iNKT cells, and the important roles it plays in hepatotoxicity. ER stress inhibitor, 4-phenylbutyrate (4-PBA), also suppressed iNKT cell activation and liver injury, which might be regulated by the STING signaling pathway. Our results demonstrated the possible mechanisms underlying TP-induced hepatotoxicity, where the activation of cDCs and iNKT cells was stimulated by upregulated STING signaling and increased ER stress as a result of TP administration.

Xin Chen, Zixun Yu, and Cheng Nong are the co-first author.

X. Chen · Z. Yu · C. Nong · M. Zhang · L. Sun ·
L. Zhang (✉) · X. Wang (✉)
New Drug Screening Center, Jiangsu Center
for Pharmacodynamics Research and Evaluation, China
Pharmaceutical University, Nanjing 210009, China
e-mail: lyzhang@cpu.edu.cn

X. Wang
e-mail: wangxz@cpu.edu.cn

R. Xue
Reproductive Medicine Center, Department of Obstetrics
and Gynecology, The First Affiliated Hospital of Anhui
Medical University, Hefei 230022, China

Y. Zhang
Division of Biosciences, University College London,
London WC1E 6BT, UK

L. Zhang
Center for Drug Research and Development, Guangdong
Pharmaceutical University, Guangzhou 510006, China

Keywords Triptolide · Liver injury · Dendritic cell ·
Invariant natural killer T cell · STING · Endoplasmic
reticulum stress

Abbreviations

ALD Alcohol-related liver disease

ALT	Alanine transaminase
ALP	Alkaline phosphatase
APAP	Acetaminophen
α -SMA	Alpha-smooth muscle actin
AST	Aspartate transaminase
ATF4	Activating transcription factor 4
ATF6	Activating transcription factor 6
APC	Antigen-presenting cells
BDL	Bile duct ligation
cDC	Conventional dendritic cell
CHOP	C/EBP homologous protein
Con A	Concanavalin A
DC	Dendritic cell
ER	Endoplasmic reticulum
eIF2 α	Eukaryotic translation initiation factor 2 alpha
FasL	Fas ligand
GRP78	Glucose-regulated protein 78
H&E	Hematoxylin and eosin
HFD	High-fat diet
HSC	Hepatic stellate cell
iNKT cell	Invariant natural killer T cell
IRE1 α	Inositol-requiring enzyme 1 α
IRF3	IFN regulatory factor 3
LSEC	Liver sinusoidal endothelial cell
NAFLD	Nonalcoholic fatty liver disease
NASH	Nonalcoholic steatohepatitis
NPC	Nonparenchymal cell
NK cell	Natural killer cell
4-PBA	4-Phenylbutyrate
pDC	Plasmacytoid DC
PERK	PKR-like ER kinase
PRR	Pattern recognition receptor
sXBP1	Spliced X-box-binding protein
TBK1	TANK-binding kinase 1
TC	Total cholesterol
TG	Triglyceride
TGF- β 1	Transforming growth factor beta-1
TP	Triptolide
TUNEL	Terminal dUTP nick-end labeling
UPR	The unfolded protein response
WT	Wild type

Introduction

Triptolide (TP) is a powerful and promising compound that originated from the Traditional Chinese Medicines *Tripterygium wilfordii* Hook F. It shows

excellent anti-cancer, anti-fertility, and immunoregulatory efficacies. However, the clinical application of TP is hindered by its disadvantages, such as multi-organ toxicity, narrow therapeutic window, and limited water solubility (Hou et al. 2019). Hepatotoxicity is one of the most prominent side effects of TP, which is associated with its immunomodulatory effects. Multiple immunocytes participate in hepatotoxicity caused by TP. Following TP administration, hepatic neutrophils and macrophages infiltrate and become activated (Wang et al. 2018a, Wang et al. 2018c). In addition, hepatic Th17 cell expansion and Treg cell reduction contribute to Th17/Treg disequilibrium (Wang et al. 2014). Our previous study has found that TP activates invariant natural killer T (iNKT) cells in the liver. Both NKT cell depletion and iNKT cell deficiency attenuate TP-induced hepatotoxicity (Wang et al. 2018b, Zou et al. 2020). NKT cells are predominantly enriched in liver and play an important role in liver diseases via rapid abundant production of cytokines (Caballano-Infantes et al. 2021). However, our in vitro results showed that the presence of antigen-presenting cells (APCs) was required for TP-induced iNKT cell activation. Therefore, we hypothesized that dendritic cells (DCs) could activate iNKT cells, thereby participating in TP-induced hepatotoxicity.

DCs are APCs that efficiently activate NKT cells. DCs constitutively expressing CD1d can present the iNKT cell-specific ligand α GalCer and directly activate iNKT cells. DCs can also transduce innate immune signals and secrete IL-12 for indirect iNKT cell activation. Upon activation, iNKT cells in turn induce the maturation and activation of DCs, cascading the initial immune response (Keller et al. 2017). DCs are the sentinels of the hepatic local immune system. The liver DCs have the dual properties of maintaining immune homeostasis by inducing immune tolerance and rapidly responding to liver injury by inducing immune response (Castellaneta et al. 2009). In the liver, DCs can be classified into conventional DCs (cDCs) and plasmacytoid DCs (pDCs). cDCs can capture, process, and present antigens and are highly immunogenic. In contrast, pDCs contain lower levels of major histocompatibility complex class II and co-stimulatory molecules, thus, mostly related to tolerance (Liu et al. 2021). In murine model of nonalcoholic steatohepatitis (NASH),

DCs expand, mature, and activate in the liver. They can suppress Kupffer cells and neutrophils, therefore protecting against NASH. Depletion of DC notably aggravates fibro-inflammation (Henning et al. 2013). Conversely, in thioacetamide-induced chronic liver fibrosis, DCs trigger inflammation by inducing the proliferation of hepatic stellate cells (HSCs), NK cells, and T cells. In this case, DC depletion dramatically extenuates the local inflammatory milieu in fibrotic livers (Connolly et al. 2009). Therefore, the role of DC remains to be elucidated.

STING, an endoplasmic reticulum (ER) membrane protein, is highly expressed in non-parenchymal cells (NPCs) of the liver, and DCs are the main functional site of STING. Activation of STING promotes DC maturation and induces the expression of co-stimulatory molecules including CD80, CD86, and CD40, and the upregulation of inflammatory factors including type I IFNs (Chen et al. 2021, Takashima et al. 2018). After detecting exogenous/endogenous abnormal nucleic acids, STING migrates from the ER to the Golgi apparatus and recruits TANK-binding kinase 1 (TBK1). TBK1 traffics phosphorylated IFN regulatory factor 3 (IRF3) to the nucleus, enhancing type I IFN transcription. STING can also promote the release of inflammatory cytokines through NF- κ B (Zhang et al. 2019). High-fat diet (HFD)-induced activation of STING in liver NPCs triggers the proinflammatory activation status of macrophages, hepatic lipid deposition, and HSC activation. Lacking STING prevents apoptosis, metabolic dysfunction, and nonalcoholic fatty liver disease (NAFLD)/NASH-related fibro-inflammation in mice (Luo et al. 2018, Qiao et al. 2018, Yu et al. 2019). ER-stressed DCs enhance iNKT cell activation in vitro and in vivo. The PKR-like ER kinase (PERK) pathway increases CD1d-mediated antigen presentation. ER stress alters the cell surface distribution of CD1d (Bedard et al. 2019). In alcohol-related liver disease (ALD), bile duct ligation (BDL), and CCl₄-induced cirrhosis, ER stress leads to increased expression of C/EBP homologous protein (CHOP) in hepatocytes (Campos et al. 2014, Liu et al. 2018, Tamaki et al. 2008). Cholestatic cirrhosis in CHOP-deficient mice is notably ameliorated due to reduced hepatocyte death and inhibition of α -SMA and TGF- β 1 expression (Liu et al. 2018; Tamaki et al. 2008). In CCl₄-induced liver fibrosis,

STING-IRF3 links ER stress to apoptotic signaling in hepatocytes (Iracheta-Vellve et al. 2016). STING and IRF3 are significant in the development of ALD and link ER stress to the mitochondrial pathway of cell death (Petrasek et al. 2013).

In this study, our results showed that TP induced ER stress and the activation of STING signaling pathway, which resulted in the activation of cDCs and iNKT cells and thereby causing hepatotoxicity. The hepatic cDCs exhibited immunogenic phenotypes with upregulation of co-stimulatory molecules and IL-12 production, both of which had an impact on iNKT cell activation and could be pathogenic in TP-induced liver injury. STING could alter cDC phenotype and function, mediate iNKT cell activation, and thus affect the progression of liver injury. ER stress also had an impact on iNKT cell activation and hepatic damage, which might form a crosstalk with STING signaling pathway in the liver.

Material and methods

Reagents

TP (CAS: 38748–32-2, batch number: 130401, contents > 98%) was purchased from Sanleng Biotech Co., Ltd., (Guilin, China) and was reconstituted in 1, 3-propylene glycol and stored at –20 °C. Then, TP was freshly diluted to the appropriate concentrations with a 0.5% carboxymethylcellulose solution before the experiments. 4-phenylbutyrate (4-PBA, CAS: 1821–12-1, Sigma, USA) was dissolved in NaOH of equal molar mass (final pH 7.2–7.4). α -GalCer (KRN 7000, CAS: 158021–47-7, Cayman) was dissolved with DMSO to prepare a 1 mg/mL stock solution and was freshly diluted with medium to 1 μ g/mL for use. Anti-CD16/32 antibody (clone: 2.4G2) for unspecific antigen blocking, anti-CD3e-FITC antibody (clone: 145-2C11), anti-CD69-PE antibody (clone: H1.2F3), anti-IFN- γ -PE antibody (clone: XMG1.2), anti-IL-4-PE antibody (clone: 11B11), anti-IL-17-PE antibody (clone: TC11-18H10), anti-CD11c-FITC antibody (clone: HL3), and anti-IL-12(p40/p70)-PE antibody (clone: C15.6) were obtained from Becton Dickinson (San Diego, CA, USA). Anti-CD45R (B220)-APC antibody (clone: RA3-6B2) and anti-CD86 (B7-2)-PE antibody (clone: GL1) were purchased from

eBioscience (Pittsburgh, PA, USA). Anti-CD40-PE antibody (clone: 3/23) was purchased from BioLegend (San Diego, CA, USA). Mouse Th1/Th2 Cytokine Kit (CBA, Cat: 551,287) and Leukocyte Activation Cocktail with BD GolgiPlug™ (Cat: 550,583) were purchased from BD Pharmingen. Mouse CD1d-PBS-57 tetramer-APC was kindly provided by the NIH Tetramer Core Facility. PMA was purchased from Beyotime (Nanjing, China). Ionomycin calcium salt and brefeldin A were purchased from FcMACS (Nanjing, China). InVivoPlus anti-mouse IL-12 p40 (clone: C17.8) and InVivoPlus rat IgG2a isotype control anti-trinitrophenol (clone: 2A3) were obtained from BioX-Cell (West Lebanon, NH, USA). AAV8-control and AAV8-STING (10^{12} vg/mouse, i.v.) were prepared by Vigene (Jinan, China). cGAS (31,659), STING (50,494), TBK1 (3504), Phospho-IRF3 (29,047), IRF3 (4302), GRP78 (3183 s), Phospho-eIF2 α (9721 s), eIF2 α (9722 s), ATF4 (11815 s), CHOP (2895 s), cleaved caspase-3 (9661), and COX IV (11967S) were purchased from Cell Signaling Technology (MA, USA). GAPDH (60,004-1-Ig) and cytochrome c (66,264-1-Ig) were purchased from Proteintech Group (Rosemont, IL, USA). TMEM173/STING (19,851-1-AP) was purchased from Proteintech Group (Rosemont, IL, USA). GM130/GOLGA2 (NBP2-53,420) was purchased from Novus Biologicals (Centennial, CO, USA). Cytochrome C (GB11080), COX IV (GB11250), and DAPI (G1012) were purchased from Servicebio (Wuhan, China).

Animal treatment

Female C57BL/6 J mice (aged 6–8 weeks, weighed 18–20 g) were purchased from Shanghai SLAC Laboratory Animal Co.,Ltd (Shanghai, China). iNKT cell-deficient $\alpha 18^{-/-}$ mice on a C57BL/6 background (aged 6 to 10 weeks) were generously provided by Dr. Li Bai (University of Science and Technology of China). All mice were grouped as follows: (1) control group — sodium carboxymethylcellulose (CMC-Na) solution (0.5%, w/v, i.g.) was administered; (2) TP group — TP (600 $\mu\text{g}/\text{kg}/\text{d}$) was intragastric administered for 1, 3, 5, or 7 days; (3) anti-IL-12p40 and TP co-administration group — TP along with anti-IL-12p40 antibody or isotype (500 $\mu\text{g}/\text{mouse}$, i.p. 24 h before TP administration); (4) AAV-siSTING and TP co-administration group — TP was administered along with transfection

of AAV-siSTING or AAV-NC (10^{12} vg/mouse, 4 weeks before TP administration); (5) 4-PBA and TP co-administration group — TP along with 4-PBA (100 mg/kg, i.p. 30 min before TP administration) was administered. There were 6 mice in each group. Dose selection was based on the results of an acute toxicity study showing an LD₅₀ value of 1280 $\mu\text{g}/\text{kg}$ for TP administration by gavage to C57BL6 mice (Wang et al. 2008). All the mice were maintained and bred under specific pathogen-free conditions at an ambient temperature of 22 ± 2 °C with a 12:12-h cycle. The mice were given ad libitum access to water and laboratory mice maintenance diets. The animals were housed in the laboratory for 1 week prior to experiments for acclimation.

NPC isolation and labeling

The NPCs were isolated as described before (Zou et al. 2020). After being stimulated with leukocyte activation cocktail for 4–5 h (BD Pharmingen), the NPCs were blocked with anti-CD16/32 and then surface-labeled by fluorescently bound anti-mouse CD3e, CD1d, CD69, CD11c, B220, CD40, and CD86 antibody staining. NPCs were fixed and permeabilized using Cytoperm/Cytofix (Becton Dickinson), and intracellular staining was performed by IFN- γ , IL-4, IL-17, or IL-12 antibody incubation. Cells were examined using a BD FACS Calibur flow cytometer. The results were processed using FlowJo version 10 software (FlowJo, Ashland, OR, USA). A total of 50,000 events were collected per tube.

Serum biochemical assays

Anticoagulant-free serum was collected, and then the levels of alanine transaminase (ALT), aspartate transaminase (AST), and alkaline phosphatase (ALP) were assessed using the ALT, AST, and ALP quantification kit (Whitman Biotech, Nanjing, China). Total cholesterol (TC) and triglyceride (TG) were measured using TC and TG quantification kit (Jiancheng Bioengineering Institute, Nanjing, China).

Hematoxylin and eosin (H&E) staining and immunohistochemistry

Liver paraffin-embedded sections were stained with H&E for histopathological examination. To detect

apoptosis, other paraffin-embedded sections were immunostained using a terminal dUTP nick-end labeling (TUNEL) detection kit (KeyGEN BioTECH, Nanjing, China) or with cleaved caspase-3. Frozen liver sections were assessed for lipid accumulation by oil red staining performed by Servicebio (Wuhan, China).

Cell culture and cell viability assay

The mouse iNKT cell hybridoma line DN32.D3 and rat RBL-CD1d cells were kindly provided by Dr. Li Bai. TP was dissolved with DMSO to prepare a 10-mM stock solution, and was freshly diluted with medium to the indicated concentrations for use. RBL-CD1d cells were cultured in 96-well plates with a concentration of 4.5×10^4 cells/mL/well or in 6-well plates with a concentration of 4.5×10^5 cells/mL/well and cultured for 12 h (at 6 h, 0.625 mM 4-PBA and DN32.D3 cells were seeded in 96-well plates with a concentration of 2.5×10^4 cells/mL/well or in 6-well plates with a concentration of 2.5×10^5 cells/mL/well). Then, the medium was removed, and the cells

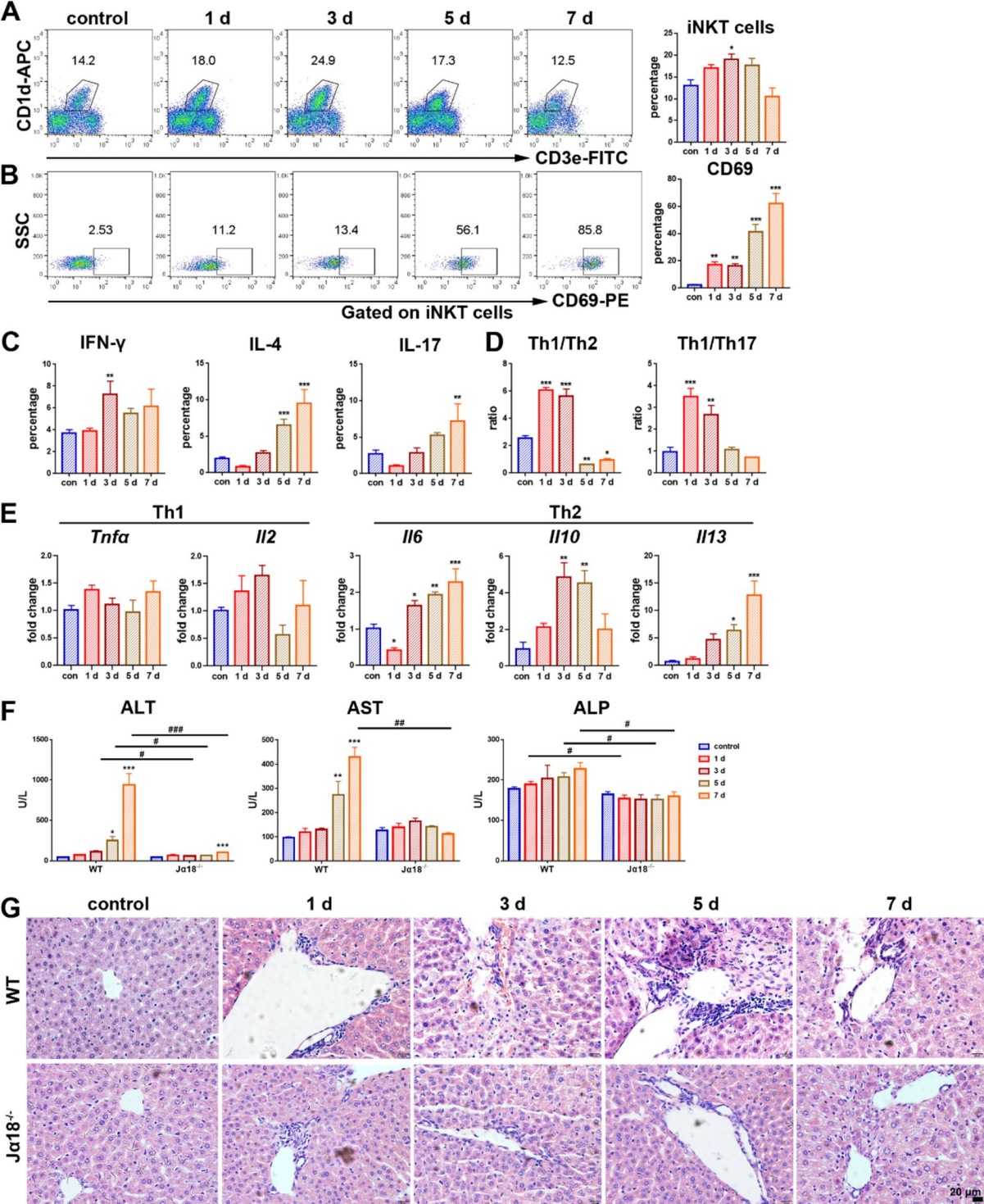
were washed with 37 °C preheated $1 \times$ PBS twice, following by adding TP. After 16 h, cells or supernatant were collected for subsequent experiments. Cell viability of exponentially growing cells was detected using CCK8 in the 96-well plates. At the indicated time, replaced the previous media with FBS-free media and different concentrations of drugs followed by CCK8 assay.

Flow cytometry analysis and CBA in vitro

In the co-culture system, cells were stimulated with either leukocyte activation cocktail or PMA and ion for 4–5 h (BD Pharmingen) before harvest. After cocktail stimulation, DN32.D3 cells were obtained by aspiration of the cell suspension from the co-culture system and stained with fluorescently bound anti-mouse CD69, IFN- γ , IL-4, or IL-17 antibody as described before. After PMA and ion stimulation, cell supernatant was obtained for CBA assay according to the instructions. The cells or supernatants were examined using a BD FACS Calibur flow cytometer. The results were processed using FlowJo version 10

Table 1 The primer sequences used for qPCR assay in vivo and in vitro

Gene	Forward (5' to 3')	Reverse (5' to 3')
<i>18S</i>	TAGAGGGACAAGTGGCGTTC	CGCTGAGCCAGTCAGTGT
<i>Atf4</i>	AACCTCATGGGTTCTCCAGCGA	CTCCAACATCCAATCTGTCCCG
<i>Atf6</i>	GTCCAAAGCGAAGAGCTGTCTG	AGAGATGCCTCCTCTGATTGGC
<i>Cd11b</i>	CGGTAGCATCAACAACAT	GCATCAAAGAGAACAAGGT
<i>Cd68</i>	GCCCGAGTACAGTCTACCTGG	AGAGATGAATTCTGCGCCAT
<i>Cgas</i>	AGAAGGACTACCTATTCAAGGCT	GGGTACGAGATAAAACGGCTC
<i>Chop</i>	GGAGGTCTGTCTCAGATGAA	GCTCCTCTGTCAGCCAAGCTAG
<i>COX I</i>	GCCCCAGATATAGCATTCCC	GTTTCATCCTGTTCTCTGCTCC
<i>Cytochrome c</i>	AGGCAAGCATAAGACTGGACC	TCTCCCCAGGTGATGCCTTTG
<i>F4/80</i>	CTTTGGCTATGGGCTTCCAGTC	GGCAAGGAGGACAGAGTTTATCGTG
<i>Gapdh</i>	AGGTCGGTGTGAACGGATTTG	GGGGTTCGTTGATGGCAACA
<i>Ifna</i>	GTGAGGAAATACTTCCACAGGATCAC	TCTCCAGACTTCTGCTCTGACCA
<i>Ifnb</i>	CTCACCTACAGGGCGGACT	GGCAAAGGCAGTGTAACTCTT
<i>Il2</i>	CCTGAAACTCCCCAGGATGC	ATGTGTTGTGTCAGAGCCCTTAGT
<i>Il6</i>	CTGCAAGAGACTTCCATCCAG	AGTGGTATAGACAGGTCTGTTGG
<i>Il10</i>	GCTGGACAACATACTGCTAACCC	ATTTCGGATAAGGCTTGCCAA
<i>Il13</i>	CCTGGCTCTTGCTTGCCTT	GGTCTTGTTGATGTTGCTCA
<i>Irf3</i>	GCGGGACTTCGTACATCTGG	TTCGGTAGGTTTCTCGGGAG
<i>Sting</i>	CTACATTGGTACTTGCGGTT	GCACCACTGAGCATGTTGTTATG
<i>Tbk1</i>	GGAGCCGTCCAATGCGTAT	GCCGTTCTCTCGGAGATGATTC
<i>Tnfa</i>	CAGGCGGTGCCTATGTCTC	CGATCACCCGAAGTTTCAGTAG



◀**Fig. 1** TP activates hepatic iNKT cells, resulting in a Th1 to Th2 cytokine bias and hepatic damage. **A** The percentage and analysis of iNKT cells; **B** the percentage and analysis of CD69⁺ iNKT cells; **C** the analysis of IFN- γ ⁺ iNKT cells; IL-4⁺ iNKT cells; IL-17⁺ iNKT cells; **D** the ratio of Th1/Th2 cytokine and Th1/Th17 cytokine produced by iNKT cells; **E** the mRNA levels of Th1 type cytokines *Tnfa*, *Il2* and Th2 type cytokines *Il6*, *Il10*, and *Il13*. In C57BL/6 J mice and α 18^{-/-} mice, **F** the levels of ALT, AST, and ALP in the serum; **G** images of liver sections stained with H&E (400 \times , scale bar=20 μ m). Data are mean \pm SEM, $n=4-6$; * $P < 0.05$, ** $P < 0.01$, and *** $P < 0.001$ vs. control. # $P < 0.05$, ## $P < 0.01$, and ### $P < 0.001$ vs. WT group

software (FlowJo, Ashland, OR, USA). A total of 30,000 events were collected per tube.

Real-time PCR

RNA was extracted from liver sections with TRIzol and cDNA was synthesized using a reverse transcription kit according to the instructions (R123-01, Vazyme Biotech, Nanjing, China). A 20- μ L real-time PCR system and thermal cycling were set up according to the kit instructions (Q111-02, Vazyme Biotech). The mRNA levels of the target genes were normalized by the mRNA levels of the housekeeping gene *Gapdh*. The primer sequences used in this study are shown in Table 1.

Western blot analysis

After the proteins were extracted, their concentrations were determined by the BCA method (Beyotime Biotechnology). Proteins were separated by SDS-PAGE and transferred to PVDF membrane. The membranes were blocked with 5% bovine serum albumin (BSA) and incubated with the corresponding primary antibodies, including cGAS (62 kDa, 1:1000), STING (33, 35 kDa, 1:1000), TBK1 (84 kDa, 1:1000), Phospho-IRF3 (45–55 kDa, 1:1000), IRF3 (45–55 kDa, 1:1000), GRP78 (78 kDa, 1:1000), Phospho-eIF2 α (38 kDa, 1:1000), eIF2 α (38 kDa, 1:1000), ATF4 (49 kDa, 1:100), CHOP (27 kDa, 1:1000), and GAPDH (36 kDa, 1:10,000). The mitochondria and cytosol fraction were isolated using Mitochondria Isolation Kit (Bioss, C5032). After the same procedures above, the membranes were incubated with

cytochrome C (12 kDa, 1:20,000) and COX IV (17 kDa, 1:1500). After incubation with appropriate secondary antibodies, the blots were detected with an enhanced chemiluminescence kit.

Immunofluorescence

Paraffin-embedded sections were stained to observe the migration of STING from ER to Golgi apparatus using TMEM173/STING polyclonal antibody (green, 1:500), GM130/GOLGA2 antibody (red, 1:1000), and DAPI (blue, 2 μ g/mL). Other paraffin-embedded sections were stained to observe the translocation of cytochrome c from mitochondrion to cytoplasm using cytochrome C polyclonal antibody (green, 1:2000), COX IV polyclonal antibody (red, 1:200), and DAPI (blue, 2 μ g/mL). The staining procedure, microscopy detection, and images collection were performed by Servicebio (Wuhan, China).

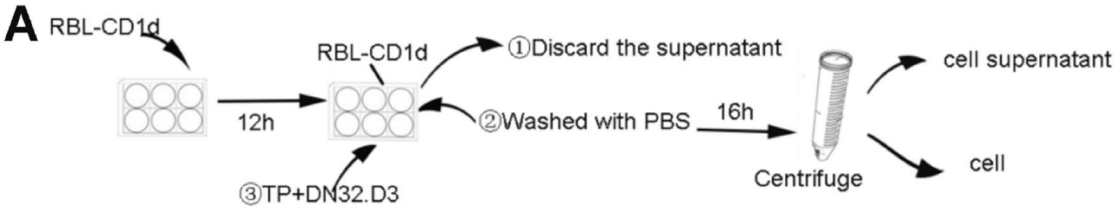
Statistical analysis

The data are expressed as mean \pm SEM. Significant differences were assessed between the two groups using Student's *t*-test and among different groups using one-way analysis of variance (ANOVA) and Dunnett's *t*-test. *P*-values < 0.05 were considered statistically significant.

Results

TP activated hepatic iNKT cells, resulting in a Th1 to Th2 cytokine bias and hepatic damage

The dynamic changes in iNKT cell activation and their cytokine secretion after TP administration were observed using the specific marker CD3^{int}CD1d-PBS-57 tetramer⁺. During TP-induced hepatotoxicity, the percentage of iNKT cells revealed a mild expansion on 3 days after TP treatment (Fig. 1A). The expression of early activation marker CD69 on iNKT cells began to increase on 1 day and a 20 to 30-fold increase was observed on 5 and 7 days, indicating a highly activated status of iNKT cells induced by TP (Fig. 1B). Among the cytokines produced by



B IC_{50} of DN32.D3 = 20.27 nM IC_{50} of RBL-CD1d = 64.93 nM

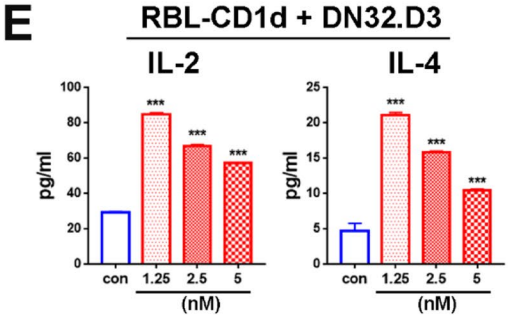
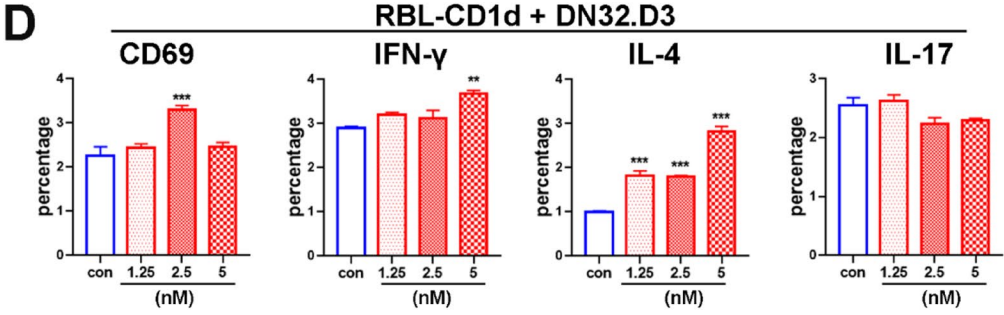
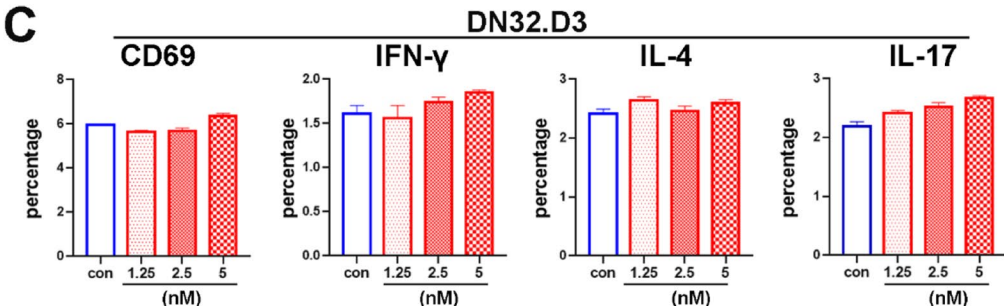
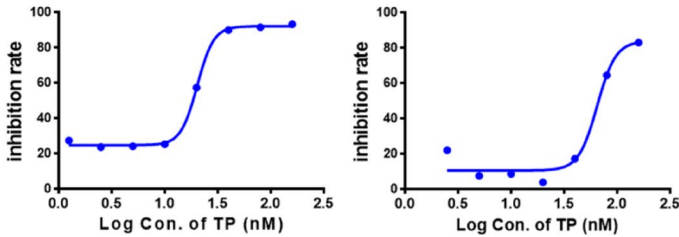


Fig. 2 TP induces the activation of iNKT cells in vitro requiring the existence of antigen presenting cells. **A** The establishment of DN32.D3 cells and RBL-CD1d cells in vitro co-culture system and the administration method of TP. **B** The IC₅₀ values of DN32.D3 cells and RBL-CD1d cells treated with TP. In DN32.D3 cells alone, **C** the expression of CD69 and production of IFN- γ , IL-4, and IL-17 by DN32.D3 cells after TP treatment. In the co-culture system, **D** the levels of CD69 and IFN- γ , IL-4, and IL-17 production of DN32.D3 cells, **E** the production of IL-2 and IL-4 in the supernatant that were measured by CBA. Data are mean \pm SEM, $n=3-6$. * $P < 0.05$, ** $P < 0.01$, and *** $P < 0.001$ vs. control

iNKT cells, an elevation of IFN- γ level was seen on 3 days, and a substantial increase in IL-4 level was observed on 5 and 7 days. In addition, IL-17 level also increased mildly on 7 days (Fig. 1C). The Th1/Th2 cytokine ratio of iNKT cells rose on 1 and 3 days and diminished on 5 and 7 days; the Th1/Th17 cytokine ratio of iNKT cells increased on 1 and 3 days and did not significantly alter on 5 and 7 days (Fig. 1D). Furthermore, the expressions of genes encoding Th1-type cytokines (*Tnfa* and *Il2*) showed no significant change after the administration of TP, while the expressions of Th2-type cytokine genes *Il6*, *Il10*, *Il13* increased constantly from 3 to 7 days (Fig. 1E). The results above demonstrated that the hepatic cytokine shifted to Th2 bias on 5 and 7 days. In the meantime, TP-induced liver injury significantly increased (Fig. 1F). To elucidate the effects of iNKT cells on TP-induced hepatotoxicity, same treatment was applied to iNKT cell-deficient $J\alpha 18^{-/-}$ mice. The results showed that TP caused serum levels of ALT and AST to increase on 5 and 7 days. In comparison to wild type (WT) group, iNKT cell-deficient mice showed lower blood biochemistry after TP treatment (Fig. 1F). Hepatic sections showed infiltration of inflammatory cells and proliferation of the pseudocholeangiolar duct and cellular degenerative edema using H&E staining. Pathology was obviously ameliorated in $J\alpha 18^{-/-}$ mice, indicating that iNKT cell-deficiency protected mice from TP-induced liver damage (Fig. 1G). Overall, these findings indicated that TP stimulated iNKT cell activation, resulting in an alteration of hepatic cytokines from Th1 to Th2 bias and leading to liver injury.

TP-induced iNKT cell activation required the presence of DCs

An in vitro co-culture system was established using the mouse iNKT cell hybridoma line DN32.D3 and

rat RBL-CD1d cells under nontoxic concentrations to examine the effects of TP (Fig. 2A and B). TP was unable to cause the activation of DN32.D3 cells alone (Fig. 2C). In the co-culture system, TP triggered the in vitro activation of iNKT cell line with upregulated surface CD69 expression and increased IFN- γ and IL-4 secretion, while IL-17 secretion remained insignificant (Fig. 2D). CBA results showed that TP induced the increased IL-2 and IL-4 production in the supernatant (Fig. 2E). IL-2 is a marker of DN32.D3 cell activation. Other cytokines were below the detection threshold and were not shown in the figure. These results showed that the activation of DN32.D3 cells induced by TP required the presence of RBL-CD1d cells and highlighted that TP-induced iNKT cell activation was dependent on its effects on APCs. Interestingly, activation of DN32.D3 cells by TP did not require α -GalCer, indicating that TP-triggered iNKT cell activation might involve an indirect activation process that is independent of CD1d.

In the present study, DCs were hypothesized to be the major APCs that activate iNKT cells and participate in the pathology. During TP-induced hepatotoxicity, the hepatic percentage of cDCs (lower right) augmented on 1 day and decreased on 7 days while the percentage of pDCs (upper right) increased on 7 days (Fig. 3A and B), indicating a transformation from cDCs to pDCs. Results showed that the expression levels of CD1d, CD40, and CD86 on cDCs and the release of IL-12 by cDCs increased from 5 days (Fig. 3C and D), representing the increasing immunogenicity of cDCs. The expressions of CD40 on the surface of pDCs and the production of IL-12 by pDCs were significantly decreased, suggesting that pDCs exhibited a tolerogenic phenotype (Fig. 3E). Anti-IL-12p40 was applied to evaluate the role of IL-12p40 in iNKT cell activation and TP-induced hepatotoxicity (Fig. 3F). Compared to the isotype and TP co-administration group, the blood biochemistry and pathology images showed that after the co-administration of TP and anti-IL-12p40 not only was liver damage mitigated (Fig. 3G and H) but the secretion of IFN- γ and IL-4 by iNKT cells also declined (Fig. 3I), suggesting that anti-IL-12p40 inhibited iNKT cell activation. Therefore, the process whereby cDCs activate iNKT cells could be mediated by IL-12.

TP induced upregulation and activation of the STING signaling pathway, while inhibition of STING reduced liver injury and inhibited the activation of cDCs and iNKT cells.

In vivo, TP significantly induced the hepatic upregulation of cGAS-STING signaling pathway at the gene and protein level and promoted the expression of type I IFN, including IFN α and IFN β (Fig. 4A and B). Immunofluorescence results showed that TP promoted the translocation of STING (green) to Golgi apparatus (red), indicating that TP induced the activation of STING in murine liver (Fig. 4C). In the in vitro co-culture system, the mRNA expressions of STING signaling pathway, the phosphorylation

of IRF3, and the protein expression of TBK1 and IRF3 increased after TP administration (Fig. 4D and E). The differences in RBL-CD1d cells alone were not significant (data not shown). The results above indicated that TP induced the activation of STING-TBK1-IRF3 signaling pathway in vitro.

To reveal the effects of STING in liver injury caused by TP, AAV-siSTING was administered to the mice 4 weeks before TP administration (Fig. 4F). Compared with co-administration of AAV-NC and

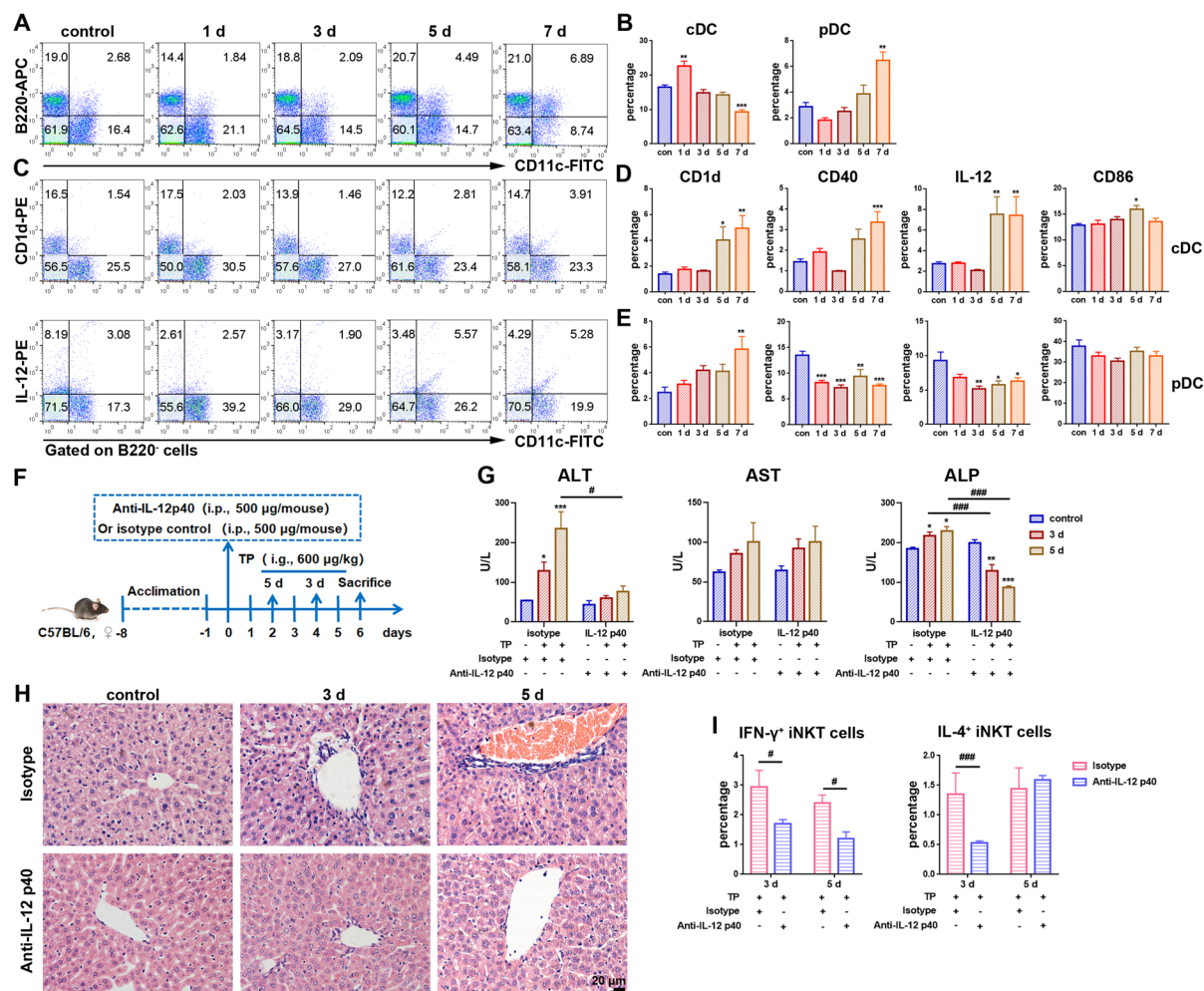


Fig. 3 TP causes the upregulation of CD1d, CD40, IL-12, and CD86 of cDCs, which contributes to the activation of iNKT cells and liver injury. **A** The percentage and **B** analysis of cDCs (lower right) and pDCs (upper right); **C** the CD1d expression on cDCs and the IL-12 production of cDCs; **D** the CD1d, CD40, and CD86 expressions on cDCs and IL-12 production by cDCs; **E** the CD1d, CD40, and CD86 expressions on pDCs and IL-12 production by pDCs. **F** The co-administra-

tion method of TP and anti-IL-12p40 antibody. **G** The serum levels of ALT, AST, and ALP. **H** Images of liver sections stained with H&E (400 \times , scale bar=20 μ m). **I** The analysis and comparison of hepatic IFN- γ + iNKT cells and IL-4+ iNKT cells. Data are mean \pm SEM, $n=4-6$; * $P<0.05$, ** $P<0.01$, and *** $P<0.001$ vs. control. # $P<0.05$, ## $P<0.01$, and ### $P<0.001$ vs. TP+isotype group

TP, serum levels of ALT, AST, and ALP decreased, and liver pathology notably ameliorated after co-administration of AAV-siSTING and TP (Fig. 4G and H), indicating the pathogenic role of STING in TP-induced hepatic damage. The expression levels of CD1d and CD40 on cDCs and the IL-12 release by cDCs were both efficiently restrained after downregulating the expression of STING (Fig. 4I), suggesting that the immunogenicity of cDCs and their capabilities for iNKT cell activation declined. The CD69 expression on iNKT cells and the secretion of IL-4 by iNKT cells were also diminished after STING expression downregulation (Fig. 4J), possibly due to a reduction in CD1d and IL-12 expression. Moreover, TP and AAV-NC co-administration inhibited the mRNA levels of *F4/80* and *Cd68* and increased the mRNA level of *Cd11b*. On the other hand, inhibiting STING expression increased the levels of *F4/80* and *Cd68* (Fig. 4K). The results above indicated that TP suppressed liver-resident macrophages and induced the monocyte-derived macrophage infiltration. Inhibiting STING expression eliminated the suppression of TP to Kupffer cells.

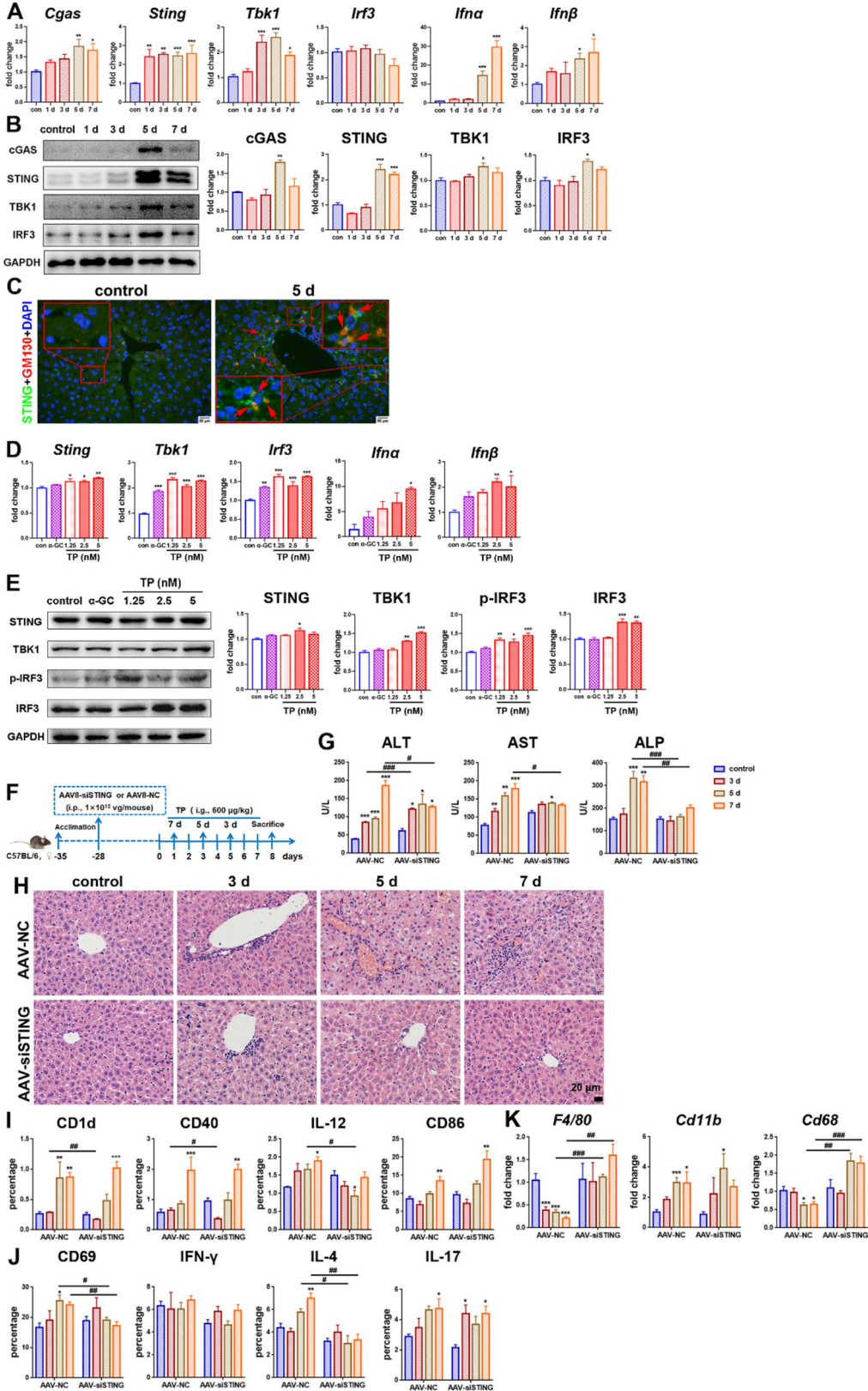
TP stimulated ER stress, and suppression of ER stress reduced hepatotoxicity and iNKT cell activation

The expression levels of glucose-regulated protein 78 (GRP78), phosphorylated eukaryotic translation initiation factor 2 α (eIF2 α), ATF4, and CHOP were significantly elevated in the WT group (Fig. 5A and B). The results indicated that TP triggered ER stress via eIF2 α -ATP4-CHOP in the liver. In contrast, the increased expression levels of the abovementioned signaling pathways were obviously downregulated in iNKT cell-deletion mice (Fig. 5A and B), indicating that TP-induced ER stress was associated with iNKT cells. Moreover, severe and persistent ER stress triggers apoptotic signaling pathway, leading to cell death (Fu et al. 2021). TP could induce pro-apoptotic activation in WT mice, as demonstrated by increased TUNEL-stained cells and elevated expression of cleaved caspase 3 (Fig. 5C and D). The control group showed that cytochrome c staining (green) was colocalized with mitochondria (red). After TP treatment, cytochrome c showed a translocation from mitochondria to cytosol (Fig. 5E, left). The protein expression of cytochrome c in mitochondria decreased, while its expression in cytosol increased (Fig. 5E, right). The

release of cytochrome c from mitochondria to cytosol could act as a trigger for caspase activation. In iNKT cell-deficient mice, changes in TUNEL staining and expression of cleaved caspase 3 were insignificant following TP administration (Fig. 5C and D). The localization and protein expression of cytochrome c in mitochondria increased, while its expression in cytosol decreased (Fig. 5E). These results suggested that iNKT cell deficiency attenuated liver apoptosis. In the co-culture system, TP also induced the upregulation of ATF4 and CHOP at 1.25 nM (Fig. 5J and K). 4-PBA, an inhibitor of ER stress, reduced the serum levels of ALT, AST, TC, and TG, and mitigated liver pathology and lipid deposition (Fig. 5G–I), suggesting that ER stress was involved in TP-induced hepatotoxicity. In the co-culture system, 4-PBA not only inhibited ATF4 and CHOP expression but also inhibited the IL-2 release by iNKT cell line compared with TP administration alone (Fig. 5J–L). IL-2 is a marker of iNKT cell line activation. These results revealed that TP-stimulated ER stress was associated with iNKT cells. In addition, suppression of ER stress ameliorated TP-induced hepatotoxicity and restrained TP-triggered iNKT cell activation. STING activation can stimulate ER stress, causing cell apoptosis (Cui et al. 2016). Downregulating STING lowered the mRNA level of *Atf6* and *Chop*, and reduced the protein levels of GRP78, ATF6, ATF4, and CHOP (Fig. 6), suggesting the potential regulatory effects of STING on ER stress. The results above revealed that TP promoted the expression of eIF2 α -ATF4-CHOP signaling pathways. ER stress contributed to iNKT cell activation and liver damage, the process of which could be modulated by STING.

Discussion

TP is an active compound that has fascinated countless researchers. Research in this field has been active, with more than one hundred publications in 2021 alone. TP endows multiple pharmacological activities and efficacies, whereas hepatotoxicity is the primary hinder for TP entering clinics. Therefore, this paper investigated the cellular and molecular mechanisms of TP-induced hepatotoxicity to explore potential targets of preventive intervention strategies. After TP administration, we observed liver iNKT cell activation and the dynamic changes in iNKT cell



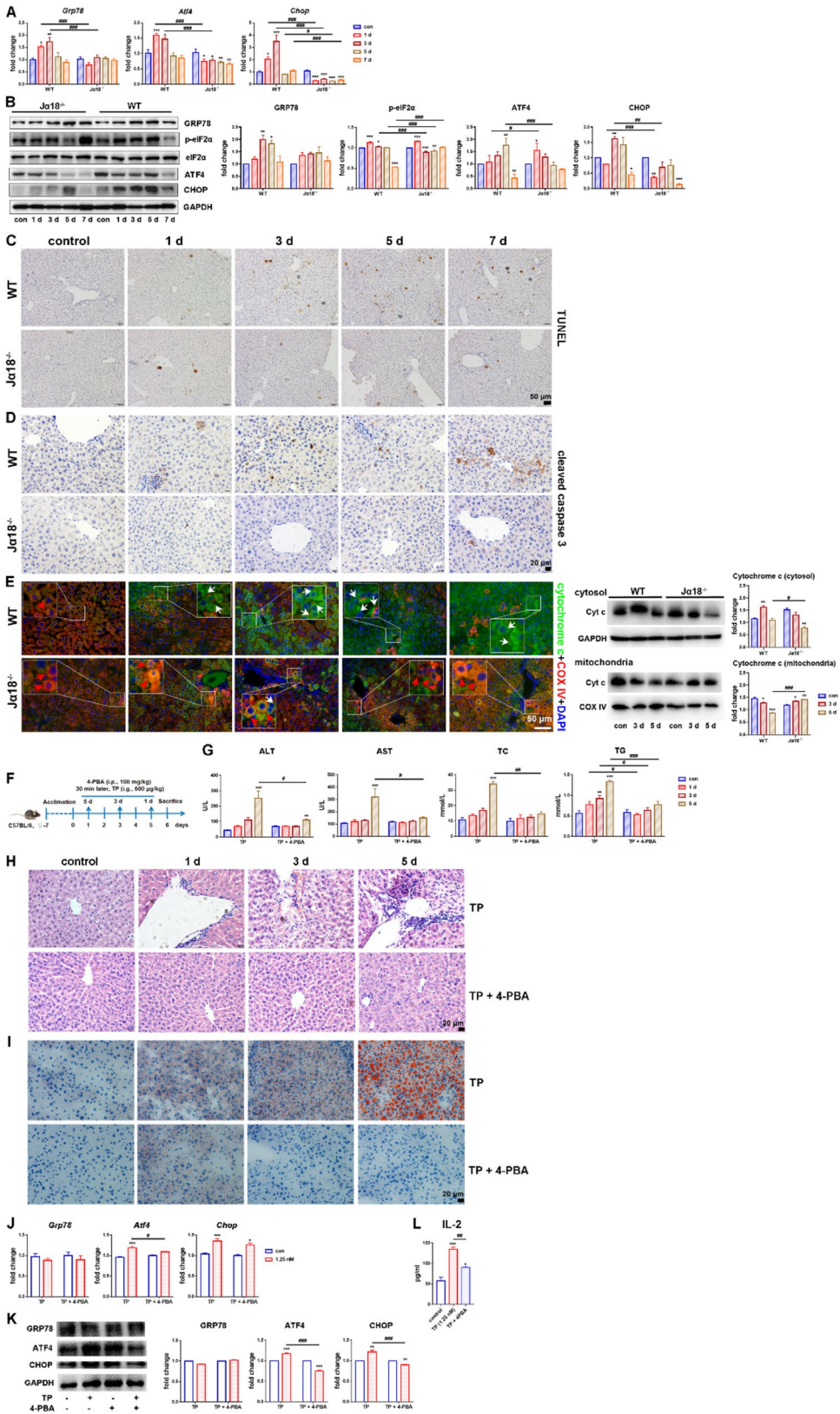
◀Fig. 4 TP activates STING signaling pathway, and inhibition of STING reduces liver injury and suppresses the activation of cDCs and iNKT cells. In murine liver, **A** the mRNA levels of STING signaling pathway; **B** the protein expressions of STING signaling pathway and the intensity of bands were normalized by GAPDH. **C** The expression and translocation of STING in liver sections. (200×, scale bar=50 μm) stained with STING (green), Golgi-specific marker (GM130, red), and nuclei (DAPI, blue). **D** the in vitro co-culture system, **E** the mRNA levels of STING signaling pathway. **F** The protein levels of STING signaling pathway and the intensity of bands were normalized by GAPDH. **G** The co-administration method of TP with AAV-NC or AAV-siSTING. **H** The serum levels of ALT, AST, and ALP. **I** Images of liver sections stained with H&E (400×, scale bar=20 μm). **J** The analysis and comparison of the CD1d, CD40, and CD86 expressions on cDCs and the IL-12 production by cDCs. **K** The analysis and comparison of hepatic CD69⁺ iNKT cells, IFN-γ⁺ iNKT cells, IL-4⁺ iNKT cells, and IL-17⁺ iNKT cells. **L** Hepatic mRNA levels of *F4/80*, *Cd11b*, and *Cd68*. Data are mean ± SEM, *n*=4–6. **P*<0.05, ***P*<0.01, and ****P*<0.001 vs. control. #*P*<0.05, ##*P*<0.01, and ###*P*<0.001 vs. TP+AAV-NC group

cytokine secretion, shifting from Th1-type to Th2-type cytokine bias. In vitro, TP-induced activation of iNKT cell line required the presence of APCs. The phenotypes and functions of hepatic DCs were therefore evaluated. cDCs exhibited an immunogenic phenotype and produced IL-12. The immunogenic cDCs played a detrimental role in TP-induced hepatic damage and promoted the activation of iNKT cells. pDCs presented a tolerogenic phenotype. TP activated STING signaling pathway while STING suppression affected the immunogenicity of cDCs, iNKT cell activation, and liver injury. TP also triggered ER stress and apoptosis. Inhibition of ER stress influenced the activation of iNKT cells and hepatic damage, which might be regulated by STING.

iNKT cells can secrete IFN-γ, IL-4, and IL-17, namely Th1, Th2, and Th17 type cytokines. The pleiotropic effects of iNKT cells are based on their cytokine production. The roles of different cytokines produced by iNKT cells in liver disease remain to be elucidated. IFN-γ has been considered to be cytotoxic and pro-inflammatory while IL-4 is protective and anti-inflammatory. However, intravenous injection of α-GalCer rapidly induces iNKT cells to produce IL-4, bringing about neutrophil accumulation and inflammation in liver and aggravating liver injury, while IFN-γ is released later, eliciting neutrophil apoptosis and mitigating hepatitis (Wang et al. 2013). In concanavalin A (Con A)-induced liver injury, IL-4 produced by iNKT cell is detrimental as it could

upregulate the expression of granzyme B and Fas ligand (FasL) and enhance cytotoxicity (Kaneko et al. 2000). Elevated IL-17 levels are thought to induce liver inflammation and liver injury. Overexpression of IL-17 by hepatic CD4⁺T and NKT cells results in massive hepatocyte necrosis in Con A-induced hepatotoxicity murine model (Yan et al. 2012). NKT cells are a novel origin of IL-17. In αGalCer-induced NKT cell-driven hepatitis model, IL-17 is predominantly derived from NKT cells rather than CD4⁺T cells. However, IL-17 produced by NKT cells attenuate inflammation (Wondimu et al. 2010). Our results showed that hepatic iNKT cells were activated with upregulated surface CD69 expression and production of IFN-γ, IL-4, and IL-17 after TP administration. Among three cytokines, IFN-γ and IL-17 secretion was increased mildly on 1 and 7 days, respectively. IL-4 secretion was massively increased on 5 and 7 days (Fig. 1C), which was parallel to the elevated serum ALT and AST levels (Fig. 1F). Th1(IFN-γ)/Th2(IL-4) ratios were also profoundly decreased on 5 and 7 days (Fig. 1D), indicating that IL-4 made a predominant contribution to the liver immune microenvironment. Moreover, the hepatic expression of Th1-type cytokine genes *Tnfα* and *Il2* showed insignificant changes, while that of Th2-type cytokine genes *Il6*, *Il10*, and *Il13* increased (Fig. 1E), further suggesting that the liver immune microenvironment was skewed to Th2 bias. iNKT cell deletion efficiently alleviated liver damage (Fig. 1F and G), suggesting that IL-4⁺ iNKT cells may have harmful effects on TP-induced hepatotoxicity. The in vitro results suggested that the activation of iNKT cell line required the presence of APCs. The primary cytokines released by iNKT cell line DN32.D3 after TP treatment were IL-2 and IL-4 (Fig. 2C–E). IL-2 is the activation marker of DN32.D3 cells and the increase in IL-4 further verified that IL-4 might be the main effector cytokine induced by TP.

To further investigate the possible hepatic APCs that activate iNKT cells, the phenotype and cytokine production of hepatic DCs were investigated. DCs can efficiently activate NKT cells. DCs can potentially present αGalCer to directly activate iNKT cells and can also secrete IL-12 to indirectly activate iNKT cells. Upon activation, iNKT cells in turn induce the maturation and activation of DCs, forming a bidirectional crosstalk (Keller et al. 2017). Although CD1d is crucial for iNKT cell activation, declined CD1d



◀Fig. 5 TP triggers hepatic ER stress, and suppressing ER stress ameliorates TP-induced hepatotoxicity and inhibits iNKT cell activation. In C57BL/6J mice and $\alpha 18^{-/-}$ mice, **A** the mRNA levels of *Grp78*, *Atf4*, and *Chop*. **B** The protein expressions of GRP78, phosphorylated eIF2 α , eIF2 α , ATF4, CHOP, and GAPDH and the intensity of bands were normalized by GAPDH. **C** TUNEL staining (200 \times , scale bar=50 μ m). **D** Immunohistochemistry of cleaved caspase-3 (400 \times , scale bar=20 μ m). **E** Immunofluorescence of cytochrome c (200 \times , scale bar=100 μ m) stained with cytochrome c (green), mitochondria marker (COX IV, red), and nuclei (DAPI, blue) and the protein expression of cytochrome c whose intensity was normalized by GAPDH or COX IV. **F** The co-administration method of TP with 4-PBA. **G** The levels of ALT, AST, TC, and TG in the serum; **H** images of liver sections stained with H&E (400 \times , scale bar=20 μ m) and **I** oil red (100 \times , scale bar=20 μ m). In the in vitro co-culture system, **J** the mRNA levels of ERS. **K** The protein levels of ERS pathway and the intensity of bands were normalized by GAPDH. **L** The analysis and comparisons of IL-2 secretion of DN32.D3 cells. Data are mean \pm SEM, $n=3-6$. * $P<0.05$, ** $P<0.01$, and *** $P<0.001$ vs. control. # $P<0.05$, ## $P<0.01$, and ### $P<0.001$ vs. WT or TP group

level on DCs is ineffective to affect the activation of iNKT cells, highlighting the importance of indirect activation (Li et al. 2019). IL-12 can work as potent as glycolipid antigens to indirectly activate iNKT cells (Brennan et al. 2013, Nagarajan and Kronenberg 2007). The IFN- γ secretion by iNKT cells requires CD40-CD40L interaction, and the IL-4 secretion by iNKT cells depends on IL-12 release and CD80/CD86-CD28 interaction (Keller et al. 2017). Among the hepatic APCs, only the surface of DCs expresses CD40 and the CD40-CD40L ligation stimulates IL-12 secretion by DCs (Keller et al. 2017). Our results indicated that after TP administration, hepatic cDCs exhibited immunogenicity with upregulated expressions of CD1d, CD40, and CD86 along with the pro-inflammatory IL-12 release (Fig. 3C and D), which contributed to both the direct and the indirect activation of iNKT cells and the IFN- γ /IL-4 production. Hepatic pDCs acted as tolerogenic DCs with suppressed levels of co-stimulatory molecules CD40 and IL-12 (Fig. 3E). Liver B220⁺ CD11c^{int} subset are identified as pDCs, and pDCs appear to be immature and tolerogenic upon stimulation (Jomantaite et al. 2004). The augmentation of cDCs on 1 day could play an early pathogenic role and the expansion of pDCs on 7 days might elicit a late protective function (Fig. 3A and B). In ConA-induced hepatitis, depletion of cDCs profoundly attenuated hepatic damage while the subsequent administration of IL-12 reinduces the

liver injury, indicating hepatic cDCs exerts harmful effects via IL-12 release. Intriguingly, IL-12 produced by DCs only influences the activation of NKT cells but not that of CD4⁺T cells, which is possibly due to the different threshold of stimuli (Wang et al. 2017). Anti-IL-12 lowers serum IFN- γ and ALT levels in liver damage model of ConA (Nicoletti et al. 2000, Wang et al. 2017). IL-12 promotes IL-4 release by iNKT cells and affects the severity of autoimmune hepatitis in a murine model (Zhu et al. 2007). In the present study, neutralization with anti-IL-12p40 antibody prevented the liver damage triggered by TP and diminished IFN- γ and IL-4 secretion by iNKT cells (Fig. 3G–I). These results suggested that IL-12 induced iNKT cell activation, which led to TP-induced hepatotoxicity.

STING is a kind of pattern recognition receptor (PRR) which recognizes abnormal nuclear acids and modulates the initiation of innate immune response in multiple pathologies. Activation of STING stimulates the IRF3 and NF- κ B signaling pathways, triggering the production of type I IFNs and diverse pro-inflammatory cytokines (Barber 2015). cGAS-STING signaling pathway contributes to acute and chronic liver diseases, including ionizing radiation-induced liver injury (Du et al. 2021), NAFLD, HFD-induced metabolic dysfunction (Bai et al. 2017, Luo et al. 2018), and ischemia–reperfusion liver injury (Zhong et al. 2020). The results indicated that TP administration promoted the translocation of STING from ER to Golgi apparatus and the expression of type I IFNs in the mouse liver (Fig. 4A–C). In the in vitro co-culture system, TP induced the phosphorylation of IRF3 and upregulation of type I IFNs (Fig. 4D and E), indicating that TP promoted the activation of STING signaling pathway in vivo and in vitro. DCs are one of the main functional sites of STING. Activation of STING induces DC maturation, upregulation of CD80/CD86, CD40, and release of type I IFNs together with other inflammatory cytokines (Chen et al. 2021; Takashima et al. 2018). Therefore, the activation of STING signaling pathway may be related to the immunogenicity of cDCs. AAV-mediated downregulation of STING decreased the CD1d, CD40 surface expression, and IL-12 production of cDCs. STING downregulation also reduced the CD69 expression and IL-4 secretion of iNKT cells (Fig. 4I and J). Moreover, STING is also expressed in hepatic NPCs, including innate immune cells Kupffer cells (Wang et al. 2021), HSC, liver sinusoidal endothelial cell (LSEC),

and adaptive immune cells (Couillin and Riteau 2021). TP and AAV-NC co-administration inhibited the mRNA expression of *F4/80* and *Cd68* and increased the mRNA level of *Cd11b*, while inhibiting STING expression increased the mRNA expression of *F4/80* and *Cd68* (Fig. 4K). Hepatic macrophages ($F4/80^+$) can be divided into Kupffer cells ($CD68^+$) and macrophages from circulation ($CD11b^+$) (Wang et al. 2018a). The results above indicated that TP could suppress liver-resident macrophages and induce the monocyte-derived macrophage infiltration. Our previous research has shown that TP induces the recruitment of macrophages ($F4/80^+CD11b^+$) and that the percentage of hepatic infiltrating macrophages, which is dependent on NKT cells, can be significantly lowered by anti-NK1.1 antibody. The present study revealed that inhibiting STING expression eliminated the TP-induced suppression of Kupffer cells. STING deficiency relieves obesity-related inflammation and insulin resistance (Mao et al. 2017). STING deletion in macrophages mitigates NAFLD-related fibro-inflammation (Luo et al. 2018). Emodin ameliorates acetaminophen-induced inflammation and hepatocyte apoptosis through suppressing the expression levels of cGA-STING signaling pathway, indicating that inhibition of STING can elicit hepatoprotective effects (Shen et al. 2021). Our results showed that suppression

of STING ameliorated TP-induced hepatotoxicity (Fig. 4G and H). The results above revealed that STING downregulation suppressed the immunogenicity of cDCs and their abilities to activate iNKT cells. STING downregulation also inhibited the activation of iNKT cells and reduced TP-induced liver injury.

ER-stressed APCs can enhance iNKT cell activation in vitro and in vivo. The enhancement is promoted by the synthesis and presentation of CD1d-presenting endogenous lipid and by the redistribution of CD1d on the cell surface. ER stress within APCs appears to be CD1d-dependent. Moreover, ER stressed APCs produce very few cytokines without iNKT cells, indicating that the ER stress forms an important link between DCs and iNKT cells (Govindarajan et al. 2020). Our results showed that TP stimulated hepatic ER stress with the enhanced expression levels of GRP78, phosphorylated eIF2 α , ATF4, and CHOP. iNKT cell deficiency suppressed ER stress in the liver (Fig. 5A and B), particularly lowering the expression of CHOP, indicating that iNKT cells also affected ER stress. GRP78 is an ER chaperone that physiologically binds to the unfolded protein response (UPR) sensor, PERK, inositol-requiring enzyme 1 (IRE1), and activating transcription

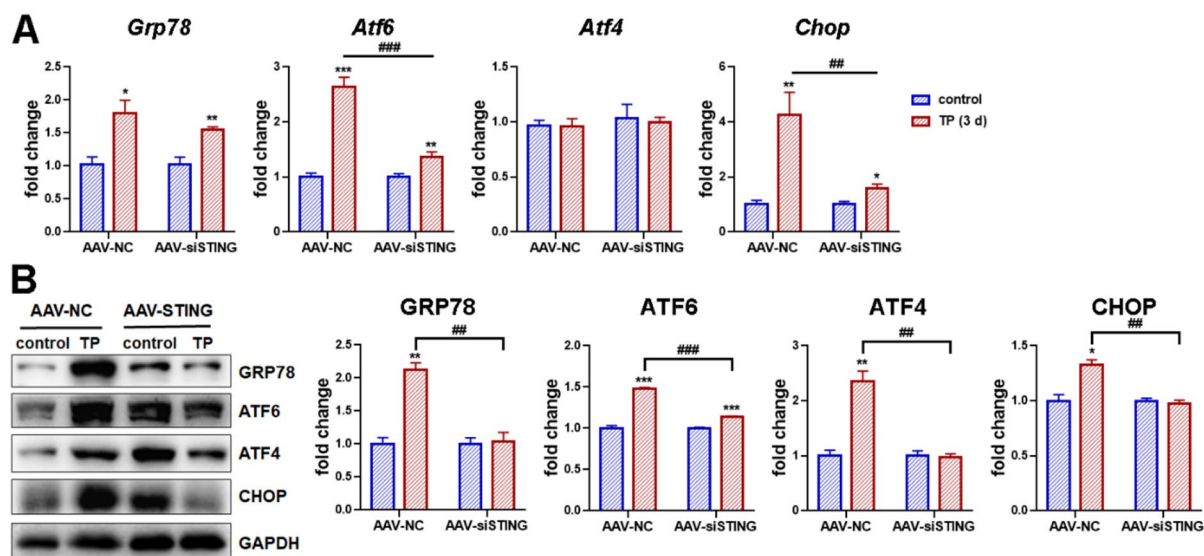


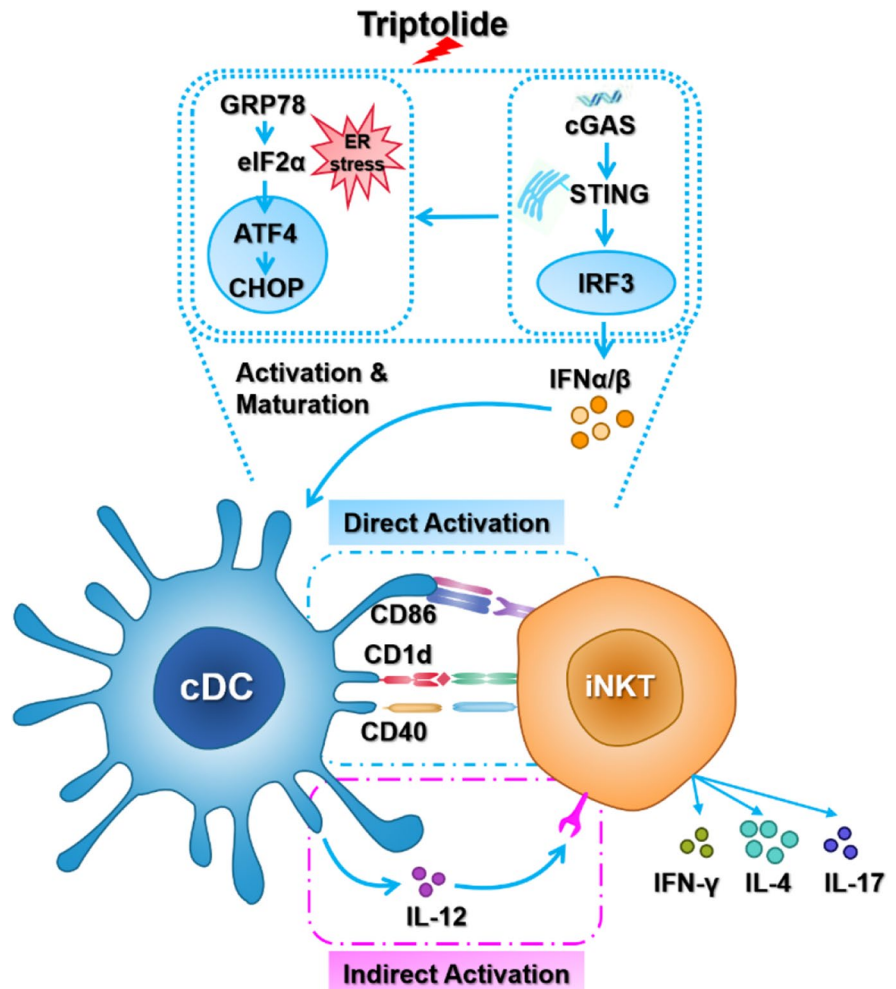
Fig. 6 Downregulation of STING inhibits the upregulated expressions of ER stress signaling pathway. **A** and **B** The mRNA, protein levels of ERS signaling pathway in the livers of co-administration of TP with AAV-NC or AAV-

siSTING and the intensity of bands were normalized by GAPDH. Data are mean \pm SEM, $n=6$. * $P<0.05$, ** $P<0.01$, and *** $P<0.001$ vs. control. # $P<0.05$, ## $P<0.01$, and ### $P<0.001$ vs. TP+AAV-NC group

factor 6 (ATF6). When misfolded protein accumulates within ER, GRP78 binds to it and simultaneously releases PERK, IRE1, and ATF6. Then, ATF6 either interacts directly with ATF4 or acts on it indirectly via spliced X-box-binding protein (sXBP1) to activate the apoptotic signaling cascade of CHOP. PERK-ATF4-CHOP is also a common pathway for cell apoptosis. The released PERK then phosphorylates eIF2 α , which upregulates the synthesis of ATF4. The ATF4 then interacts with CHOP to initiate apoptosis (Walter and Ron 2011). If ER stress is insufficiently resolved, the cells will inevitably undergo apoptosis (Fu et al. 2021). The TUNEL staining, cleaved caspase-3 upregulation, and migration of cytochrome c from mitochondria to cytoplasm revealed the pro-apoptotic activation induced by TP, while iNKT cell-deficient mice

showed alleviated liver apoptosis induced by TP (Fig. 5C–E). Persistent ER stress causes liver diseases by inducing steatosis and cell death (Malhi and Kaufman 2011). In the present study, using ER stress inhibitor extenuated TP-induced liver damage and lipid deposition by suppressing the activation of iNKT cells (Fig. 5G–L). ER stress is indispensable for the mRNA stability of cytokines produced by iNKT cells. IRE1 α ablation in iNKT cells diminishes the cytokine release and prevents the murine colitis (Govindarajan et al. 2018). In the early phase of ALD, ethanol causes ER stress and activates IRF3 with STING, which induces the subsequent cell apoptosis. STING deficiency suppresses IRF3 phosphorylation by ethanol or ER stress (Petrasek et al. 2013). In acute fibrosis induced by CCl₄, ER stress and apoptosis are regulated by STING-IRF3

Fig. 7 Graphical abstract



(Iracheta-Vellve et al. 2016). These studies demonstrate that STING signaling pathway and ER stress crosstalk and participate in cell death, steatosis, and the development of liver injury. Our results revealed that downregulating STING expression suppressed hepatic ER stress (Fig. 6A and B), indicating that STING may regulate ER stress.

Conclusion

In summary, we investigated the dynamic alterations of hepatic iNKT cell activation and cDC activation during TP-induced hepatic damage. After TP administration, IL-4 secretion by iNKT cells was significantly increased, in parallel to the liver injury. In the *in vitro* co-culture system, TP-induced iNKT cell line activation required the presence of APCs. The activated iNKT cells mainly secreted IL-4. cDCs exerted immunogenic effects via an upregulation of CD1d, CD40, CD86, and IL-12 production. These were detrimental in TP-induced liver damage and affected both the direct and the indirect activation of iNKT cells. pDCs, on the other hand, were shown to be tolerogenic. STING affected iNKT cell activation and TP-induced hepatotoxicity, possibly via altering the phenotype of cDCs and their ability to activate iNKT cells. ER stress influenced iNKT cell activation and TP-induced hepatic damage, which might form a crosstalk with STING (Fig. 7). These results shed lights on the mechanisms of TP-induced hepatotoxicity and potential therapeutic targets to prevent hepatotoxicity.

Acknowledgements The authors would like to acknowledge Li Bai (University of Science and Technology of China) for kindly providing iNKT cell-deficient ($J\alpha 18^{-/-}$ mice), DN32. D3 cells, and RBL-CD1d cells. The authors also would like to acknowledge NIH Tetramer Core Facility for generously providing mouse CD1d-PBS-57 tetramer-APC. The authors would appreciate Zhenglin Hao, who works in the Pharmaceutical Animal Experimental Center of China Pharmaceutical University, for his kind help with *in vivo* experiments.

Author contribution Z.Y., N.C., and X.C. performed the experiments, collected data, and analyzed the data. X.C., X.W., M.Z., and L.S. completed the revision experiments. L.Z. and X.W. contributed to the guidance of experiments and the final manuscript. X.R., L.Z., and X.W. designed the study. X.W. wrote the manuscript and answered the reviewers' questions. Y.Z. modified the language throughout the text. All the authors reviewed the manuscript.

Funding The present study was supported by the National Natural Science Foundation of China (No. 81703626, No. 82073948, No. 81973562), and National Innovation and Entrepreneurship Training Program for Undergraduate (No. 202210316040Z).

Data availability The datasets generated or analyzed during the current study are available from the corresponding author on reasonable request.

Declarations

Ethical approval All procedures involved in this study were approved by the Ethics Committee of China Pharmaceutical University and conformed to the Laboratory Animal Management Committee of Jiangsu Province guidelines (Approval No.: 2110748).

Consent to participate Not applicable.

Human ethics Not applicable.

Consent for publication All authors have agreed to publish this manuscript.

Competing interests The authors declare no competing interests.

References

- Bai J, Cervantes C, Liu J, He S, Zhou H, Zhang B, et al. DsbA-L prevents obesity-induced inflammation and insulin resistance by suppressing the mtDNA release-activated cGAS-cGAMP-STING pathway. *Proc Natl Acad Sci U S A*. 2017;114:12196–201.
- Barber GN. STING: infection, inflammation and cancer. *Nat Rev Immunol*. 2015;15:760–70.
- Bedard M, Shrestha D, Priestman DA, Wang Y, Schneider F, Matute JD, et al. Sterile activation of invariant natural killer T cells by ER-stressed antigen-presenting cells. *Proc Natl Acad Sci U S A*. 2019;116:23671–81.
- Brennan PJ, Brigl M, Brenner MB. Invariant natural killer T cells: an innate activation scheme linked to diverse effector functions. *Nat Rev Immunol*. 2013;13:101–17.
- Caballano-Infantes E, Garcia-Garcia A, Lopez-Gomez C, Cueto A, Robles-Diaz M, Ortega-Alonso A, et al. Differential iNKT and T cells activation in non-alcoholic fatty liver disease and drug-induced liver injury. *Biomed*. 2021;10:55.
- Campos G, Schmidt-Heck W, Ghallab A, Rochlitz K, Putter L, Medinas DB, et al. The transcription factor CHOP, a central component of the transcriptional regulatory network induced upon CCl4 intoxication in mouse liver, is not a critical mediator of hepatotoxicity. *Arch Toxicol*. 2014;88:1267–80.

- Castellaneta A, Sumpter TL, Chen L, Tokita D, Thomson AW. NOD2 ligation subverts IFN- α production by liver plasmacytoid dendritic cells and inhibits their T cell allostimulatory activity via B7–H1 up-regulation. *J Immunol*. 2009;183:6922–32.
- Chen C, Yang RX, Xu HG. STING and liver disease. *J Gastroenterol*. 2021;56:704–12.
- Connolly MK, Bedrosian AS, Mallen-St Clair J, Mitchell AP, Ibrahim J, Stroud A, et al. In liver fibrosis, dendritic cells govern hepatic inflammation in mice via TNF- α . *J Clin Invest*. 2009;119:3213–25.
- Couillin I, Riteau N. STING signaling and sterile inflammation. *Front Immunol*. 2021;12:753789.
- Cui Y, Zhao D, Sreevatsan S, Liu C, Yang W, Song Z, et al. *Mycobacterium bovis* induces endoplasmic reticulum stress mediated-apoptosis by activating IRF3 in a murine macrophage cell line. *Front Cell Infect Microbiol*. 2016;6:182.
- Du S, Chen G, Yuan B, Hu Y, Yang P, Chen Y, et al. DNA sensing and associated type 1 interferon signaling contributes to progression of radiation-induced liver injury. *Cell Mol Immunol*. 2021;18:1718–28.
- Fu X, Cui J, Meng X, Jiang P, Zheng Q, Zhao W, et al. Endoplasmic reticulum stress, cell death and tumor: association between endoplasmic reticulum stress and the apoptosis pathway in tumors (Review). *Oncol Rep*. 2021;45:801–8.
- Govindarajan S, Gaublotte D, Van der Cruyssen R, Verheugen E, Van Gassen S, Saeys Y, et al. Stabilization of cytokine mRNAs in iNKT cells requires the serine-threonine kinase IRE1 α . *Nat Commun*. 2018;9:5340.
- Govindarajan S, Verheugen E, Venken K, Gaublotte D, Maelegheer M, Cloots E, et al. ER stress in antigen-presenting cells promotes NKT cell activation through endogenous neutral lipids. *EMBO Rep*. 2020;21:e48927.
- Henning JR, Graffeo CS, Rehman A, Fallon NC, Zambirinis CP, Ochi A, et al. Dendritic cells limit fibroinflammatory injury in nonalcoholic steatohepatitis in mice. *Hepatology*. 2013;58:589–602.
- Hou W, Liu B, Xu H. Triptolide: medicinal chemistry, chemical biology and clinical progress. *Eur J Med Chem*. 2019;176:378–92.
- Iracheta-Vellve A, Petrasek J, Gyongyosi B, Satishchandran A, Lowe P, Kodys K, et al. Endoplasmic reticulum stress-induced hepatocellular death pathways mediate liver injury and fibrosis via stimulator of interferon genes. *J Biol Chem*. 2016;291:26794–805.
- Jomantaite I, Dikopoulos N, Kroger A, Leithauser F, Hauser H, Schirmbeck R, et al. Hepatic dendritic cell subsets in the mouse. *Eur J Immunol*. 2004;34:355–65.
- Kaneko Y, Harada M, Kawano T, Yamashita M, Shibata Y, Gejyo F, et al. Augmentation of Valpha14 NKT cell-mediated cytotoxicity by interleukin 4 in an autocrine mechanism resulting in the development of concanavalin A-induced hepatitis. *J Exp Med*. 2000;191:105–14.
- Keller CW, Freigang S, Lunemann JD. Reciprocal crosstalk between dendritic cells and natural killer T cells: mechanisms and therapeutic potential. *Front Immunol*. 2017;8:570.
- Li C, Song B, Santos PM, Butterfield LH. Hepatocellular cancer-derived alpha fetoprotein uptake reduces CD1 molecules on monocyte-derived dendritic cells. *Cell Immunol*. 2019;335:59–67.
- Liu R, Li X, Huang Z, Zhao D, Ganesh BS, Lai G, et al. C/EBP homologous protein-induced loss of intestinal epithelial stemness contributes to bile duct ligation-induced cholestatic liver injury in mice. *Hepatology*. 2018;67:1441–57.
- Liu W, Zeng X, Liu Y, Liu J, Li C, Chen L, et al. The immunological mechanisms and immune-based biomarkers of drug-induced liver injury. *Front Pharmacol*. 2021;12:723940.
- Luo X, Li H, Ma L, Zhou J, Guo X, Woo SL, et al. Expression of STING is increased in liver tissues from patients with NAFLD and promotes macrophage-mediated hepatic inflammation and fibrosis in mice. *Gastroenterology*. 2018;155(1971–84): e4.
- Malhi H, Kaufman RJ. Endoplasmic reticulum stress in liver disease. *J Hepatol*. 2011;54:795–809.
- Mao Y, Luo W, Zhang L, Wu W, Yuan L, Xu H, et al. STING-IRF3 triggers endothelial inflammation in response to free fatty acid-induced mitochondrial damage in diet-induced obesity. *Arterioscler Thromb Vasc Biol*. 2017;37:920–9.
- Nagarajan NA, Kronenberg M. Invariant NKT cells amplify the innate immune response to lipopolysaccharide. *J Immunol*. 2007;178:2706–13.
- Nicoletti F, Di Marco R, Zaccone P, Salvaggio A, Magro G, Bendtzen K, et al. Murine concanavalin A-induced hepatitis is prevented by interleukin 12 (IL-12) antibody and exacerbated by exogenous IL-12 through an interferon- γ -dependent mechanism. *Hepatology*. 2000;32:728–33.
- Petrasek J, Iracheta-Vellve A, Csak T, Satishchandran A, Kodys K, Kurt-Jones EA, et al. STING-IRF3 pathway links endoplasmic reticulum stress with hepatocyte apoptosis in early alcoholic liver disease. *Proc Natl Acad Sci U S A*. 2013;110:16544–9.
- Qiao JT, Cui C, Qing L, Wang LS, He TY, Yan F, et al. Activation of the STING-IRF3 pathway promotes hepatocyte inflammation, apoptosis and induces metabolic disorders in nonalcoholic fatty liver disease. *Metabolism*. 2018;81:13–24.
- Shen P, Han L, Chen G, Cheng Z, Liu Q. Emodin attenuates acetaminophen-induced hepatotoxicity via the cGAS-STING pathway. *Inflam*. 2021;45:74–87.
- Takashima K, Oshiumi H, Matsumoto M, Seya T. TICAM-1 is dispensable in STING-mediated innate immune responses in myeloid immune cells. *Biochem Biophys Res Commun*. 2018;499:985–91.
- Tamaki N, Hatano E, Taura K, Tada M, Kodama Y, Nitta T, et al. CHOP deficiency attenuates cholestasis-induced liver fibrosis by reduction of hepatocyte injury. *Am J Physiol Gastrointest Liver Physiol*. 2008;294:G498–505.
- Walter P, Ron D. The unfolded protein response: from stress pathway to homeostatic regulation. *Science*. 2011;334:1081–6.
- Wang Y, Jia L, Wu CY. Triptolide inhibits the differentiation of Th17 cells and suppresses collagen-induced arthritis. *Scand J Immunol*. 2008;68:383–90.
- Wang H, Feng D, Park O, Yin S, Gao B. Invariant NKT cell activation induces neutrophil accumulation and hepatitis: opposite regulation by IL-4 and IFN- γ . *Hepatology*. 2013;58:1474–85.

- Wang X, Jiang Z, Cao W, Yuan Z, Sun L, Zhang L. Th17/Treg imbalance in triptolide-induced liver injury. *Fitoterapia*. 2014;93:245–51.
- Wang J, Cao X, Zhao J, Zhao H, Wei J, Li Q, et al. Critical roles of conventional dendritic cells in promoting T cell-dependent hepatitis through regulating natural killer T cells. *Clin Exp Immunol*. 2017;188:127–37.
- Wang L, Xu D, Li L, Xing X, Liu L, Ismail Abdelmotalab M, et al. Possible role of hepatic macrophage recruitment and activation in triptolide-induced hepatotoxicity. *Toxicol Lett*. 2018a;299:32–9.
- Wang XZ, Xue RF, Zhang SY, Zheng YT, Zhang LY, Jiang ZZ. Activation of natural killer T cells contributes to triptolide-induced liver injury in mice. *Acta Pharmacol Sin*. 2018b;39:1847–54.
- Wang XZ, Zhang SY, Xu Y, Zhang LY, Jiang ZZ. The role of neutrophils in triptolide-induced liver injury. *Chin J Nat Med*. 2018c;16:653–64.
- Wang L, You HM, Meng HW, Pan XY, Chen X, Bi YH, et al. STING-mediated inflammation contributes to Gao binge ethanol feeding model. *J Cell Physiol*. 2021;237:1471–1485.
- Wondimu Z, Santodomingo-Garzon T, Le T, Swain MG. Protective role of interleukin-17 in murine NKT cell-driven acute experimental hepatitis. *Am J Pathol*. 2010;177:2334–46.
- Yan S, Wang L, Liu N, Wang Y, Chu Y. Critical role of interleukin-17/interleukin-17 receptor axis in mediating Con A-induced hepatitis. *Immunol Cell Biol*. 2012;90:421–8.
- Yu Y, Liu Y, An W, Song J, Zhang Y, Zhao X. STING-mediated inflammation in Kupffer cells contributes to progression of nonalcoholic steatohepatitis. *J Clin Invest*. 2019;129:546–55.
- Zhang C, Shang G, Gui X, Zhang X, Bai XC, Chen ZJ. Structural basis of STING binding with and phosphorylation by TBK1. *Nature*. 2019;567:394–8.
- Zhong W, Rao Z, Rao J, Han G, Wang P, Jiang T, et al. Aging aggravated liver ischemia and reperfusion injury by promoting STING-mediated NLRP3 activation in macrophages. *Aging Cell*. 2020;19:e13186.
- Zhu R, Diem S, Araujo LM, Aumeunier A, Denizeau J, Philadelphie E, et al. The Pro-Th1 cytokine IL-12 enhances IL-4 production by invariant NKT cells: relevance for T cell-mediated hepatitis. *J Immunol*. 2007;178:5435–42.
- Zou M, Nong C, Yu Z, Cai H, Jiang Z, Xue R, et al. The role of invariant natural killer T cells and associated immunoregulatory factors in triptolide-induced cholestatic liver injury. *Food Chem Toxicol*. 2020;146:111777.

Publisher's note Springer Nature remains neutral with regard to jurisdictional claims in published maps and institutional affiliations.

Springer Nature or its licensor (e.g. a society or other partner) holds exclusive rights to this article under a publishing agreement with the author(s) or other rightsholder(s); author self-archiving of the accepted manuscript version of this article is solely governed by the terms of such publishing agreement and applicable law.